

Mean field dynamo action in shear flows. I: fixed kinetic helicity

Naveen Jingade^{1,2*} and Nishant K. Singh^{3,4†}

¹Indian Institute of Science, Bangalore 560 012, India

²Raman Research Institute, Sadashivanagar, Bangalore 560 080, India

³Max Planck Institute for Solar System Research, Justus-von-Liebig-Weg 3, D-37077 Göttingen, Germany

⁴Inter-University Centre for Astronomy and Astrophysics, Post Bag 4, Ganeshkhind, Pune 411 007, India

21 August 2021

ABSTRACT

We study mean-field dynamo action in a background linear shear flow by employing pulsed renewing flows with fixed kinetic helicity and nonzero correlation time (τ). We use plane shearing waves in terms of time-dependent exact solutions to the Navier-Stokes equation as derived by Singh & Sridhar (2017). This allows us to self-consistently include the anisotropic effects of shear on the stochastic flow. We determine the average response tensor governing the evolution of mean magnetic field, and study the properties of its eigenvalues which yield the growth rate (γ) and the cycle period (P_{cyc}) of the mean magnetic field. Non-axisymmetric mode of the mean-field decay as $t \rightarrow \infty$ and hence are deemed unimportant for mean-field dynamo. Both, γ and the wavenumber corresponding to the fastest growing axisymmetric mode vary non-monotonically with shear rate S when τ is comparable to the eddy turnover time T , in which case, we also find quenching of dynamo when shear becomes too strong. When $\tau/T \sim \mathcal{O}(1)$, the cycle period (P_{cyc}) of growing dynamo wave scales with shear as $P_{\text{cyc}} \propto |S|^{-1}$ at small shear, and it becomes nearly independent of shear as shear becomes too strong. This asymptotic behaviour at weak and strong shear has implications for magnetic activity cycles of stars in recent observations. Our study thus essentially generalizes the standard $\alpha\Omega$ (or $\alpha^2\Omega$) dynamo as also the α effect is affected by shear and the modelled random flow has a finite memory.

Key words: dynamo - magnetic fields - MHD - turbulence - shear flows

1 INTRODUCTION

Coherent large-scale magnetic fields and mean differential rotation are two common features of most astrophysical objects, such as, the Sun, stars, galaxies, etc (Parker 1979; Zeldovich et al. 1983; Ruzmaikin, Shukurov & Sokoloff 1998; Jones 2011; Han 2017). Magnetic fields in these systems are maintained by turbulent dynamo action where the standard paradigm for large-scale component involves amplification of weak seed fields due to helical turbulence in shear flows (Moffatt 1978; Krause & Rädler 1980; Brandenburg & Subramanian 2005). The α effect, which, in idealized settings, is a measure of net kinetic helicity and arises naturally in systems with rotation and stratification, plays a crucial role in driving large scale dynamos in a variety of systems (e.g. Dormy & Soward 2007; Charbonneau 2010; Brandenburg et al. 2012); see also Courvoisier, Hughes & Tobias (2006); Hori & Yoshida (2008) for a more general description of the α effect, where non-local and non-instantaneous effect are considered in the expression of turbulent EMF by employing integral relation between EMF and mean-field, unlike simplified standard dynamo models where the EMF depends on the local and instantaneous value of the mean magnetic field.

Direct numerical simulations in galactic or solar contexts have shown that the large scale magnetic fields are naturally produced as a result of a mean-field turbulent dynamo in local as well as global setups, where the mirror symmetry of turbulence is

* E-mail: naveen@rri.res.in

† E-mail: nishant@iucaa.in

broken either by having a helical driving or by enabling convection in a rotating system (Brandenburg, Bigazzi & Subramanian 2001; Gressel et al. 2008; Käpylä et al. 2012; Warnecke et al. 2014; Käpylä et al. 2016, 2018). Mean shear is common to these studies and the dynamo is thought to be of $\alpha\Omega$ -type, or, more generally, of $\alpha^2\Omega$ -type as the role of α -term in the generation of shear-wise component may indeed be comparable to the Ω -effect (Viviani et al. 2019); see, e.g., Brandenburg & Subramanian (2005), for different types of dynamos. It is known that the α -effect is a more complicated tensorial object (Rädler et al. 2003; Brandenburg & Subramanian 2005), which might be much different from the net kinetic helicity of the flow (Kleeorin & Rogachevskii 2003; Chamandy & Singh 2017). Turbulent transport coefficients, such as the α -tensor, are often numerically determined in a variety of contexts (Sur et al. 2008; Mitra et al. 2009).

Somewhat less common approach to study the large-scale dynamo is to directly solve for the evolution of mean magnetic field by determining the response function for a given smooth random flow (Gilbert & Bayly 1992; Kolekar, Subramanian & Sridhar 2012). Such a model is shown to faithfully represent a fast or small-scale dynamo (Zeldovich et al. 1984; Bayly & Childress 1988; Gilbert & Bayly 1992). Essentially all astrophysical bodies are expected to host a small-scale dynamo, which appears to be always excited when the magnetic Reynolds number exceeds a critical value (Zeldovich et al. 1983). There are concerns that its presence makes the description of large-scale dynamo in terms of standard mean field magnetohydrodynamics (MHD), or, say, α -prescription, less straightforward (e.g. Schekochihin, Boldyrev & Kulsrud 2002; Courvoisier, Hughes & Tobias 2006).

Gilbert & Bayly (1992), hereafter GB92, chose random helical flows in their model where they also included the memory effects, and showed analytically that the magnetic field develops intermittency in time¹. They also found growing solutions for the first moment or the mean magnetic field, and, in the limit of small correlation times, they recovered the predictions of standard α^2 dynamo for the growth rate. Kolekar, Subramanian & Sridhar (2012), hereafter KSS12, extended the work of GB92 to also include the effect of shear, and showed quite generally, that the mean field dynamo action is not possible so long as the flows are strictly non-helical. By considering a particular model of random helical flow, they derived a generalized response tensor, which yields, for fixed kinetic helicity and small correlation times, the same dispersion relation as that from a standard $\alpha^2\Omega$ dynamo. In paper II (Jingade & Singh 2020) we consider flows with fluctuating kinetic helicity, which has a renovation time greater than the velocity renovation time, and show that the growth of mean-magnetic field is possible even in the absence of negative turbulent diffusion (Kraichnan 1976a).

Following GB92; KSS12, we adopt here a renovating flow based model which allows us to describe the evolution of mean magnetic field, without explicitly deriving any mean electromotive force (EMF) which is essential in standard mean field MHD. In this model, one assumes an exactly solvable flow field in terms of a single plane wave which renovates itself after each time interval τ . Thus, the time is split into equal intervals of length τ and the velocity fields in different intervals are assumed to be statistically independent. The evolution of magnetic field is then determined by the realization of the velocity field only in a fixed interval. Such a model neither involves any closure approximation, nor is it limited to low fluid or magnetic Reynolds numbers. KSS12 in their analysis considered forced overdamped shearing waves to model the renovating flows. Here we make use of plane shearing waves, which are time-dependent exact solutions to the Navier-Stokes equations as derived by Singh & Sridhar (2017). Shear induces anisotropy in the renovating flow, which, in this work, is allowed to freely decay for the renovation time τ , and it is reset to the same amplitude at the beginning of each renovation interval. Such a resetting essentially tries to capture the effects of a random forcing after every τ .

In Section 2 we present the model of renovating flow in a background linear shear flow and then discuss the helical shearing waves which are used in this work. Linear shear makes the induction equation inhomogeneous in the lab frame; see Eq. (9). To deal with this, we make use of shearing coordinate transformation and then determine the Cauchy's solution for ideal induction equation in shearing frame. We then derive an expression for the average response tensor governing the evolution of mean magnetic field in Fourier space after suitably averaging over randomness of the flow. Behaviour of non-axisymmetric modes of mean magnetic field is presented in Section 3. In Section 4 we present our findings on the axisymmetric mean field dynamos, where we explore various properties of dynamo growth rate and its cycle period in detail, and discuss the significance of new predictions from our model in light of recent observations. We conclude in Section 5.

2 MODEL DESCRIPTION

We, now investigate the evolution of the mean-magnetic field in the background shear flow along with the turbulence. Such systems are common in astrophysical scenario like Sun, Galaxies, accretion disk etc. Let $(\mathbf{e}_1, \mathbf{e}_2, \mathbf{e}_3)$ be the orthonormal unit vectors in the Cartesian coordinate system in the lab frame, where $\mathbf{X} = (X_1, X_2, X_3)$ is a position vector. We choose mean shear to be acting in the \mathbf{e}_2 direction (azimuthal direction), varying along X_1 linearly, which is a local shearing-sheet

¹ The term 'memory effect' is used in this work to indicate that the random flow has non-zero correlation times. As clarified in Sridhar & Singh (2014), this is equivalent to more usual notion of memory effects in dynamo theory when the turbulent EMF is affected by the time dependence of the mean magnetic field, whereas in the white-noise case, the generalized EMF with a history term through a time-integral reduces to a simple expression leading to an instantaneous relation with the mean magnetic field.

approximation to the differential rotation of the disks (Goldreich & Lynden-Bell 1965; Brandenburg et al. 2008). The model velocity field \mathbf{U} can be written as, $\mathbf{U}(\mathbf{X}, t) = S X_1 \mathbf{e}_2 + \mathbf{u}(\mathbf{X}, t)$, where \mathbf{u} is the turbulent velocity field, and the shear rate S is a constant parameter.

2.1 Renewing flows in shearing background

Let us consider the inviscid Navier–Stokes equation in the background linear shear flow for the unit mass density,

$$\left(\frac{\partial}{\partial t} + S X_1 \frac{\partial}{\partial X_2} \right) \mathbf{u} + S u_1 \mathbf{e}_2 + (\mathbf{u} \cdot \nabla) \mathbf{u} = -\nabla p, \quad \text{with} \quad \nabla \cdot \mathbf{u} = 0, \quad (1)$$

where we have also assumed the flow \mathbf{u} to be incompressible. We look for the single helical wave solution of the form,

$$\mathbf{u}(\mathbf{X}, t) = \mathbf{A}(St, \mathbf{q}) \sin(\mathbf{Q}(t) \cdot \mathbf{X} + \Psi) + h \mathbf{C}(St, \mathbf{q}) \cos(\mathbf{Q}(t) \cdot \mathbf{X} + \Psi) \quad (2)$$

where $\mathbf{Q}(t)$ is a shearing wavevector having the form $\mathbf{Q} = (q_1 - S q_2(t - t_0), q_2, q_3)$, $\mathbf{q} = (q_1, q_2, q_3)$ is the wavevector at initial time t_0 , and Ψ denotes the phase of the wave. This particular form of wave vector arises because of the inhomogeneity of the Eq. (1) in the variable X_1 . $\mathbf{A}(St, \mathbf{q})$ and $\mathbf{C}(St, \mathbf{q})$ are the amplitudes of the sheared helical wave and h controls the relative helicity of the flow. The above velocity field is supplemented by

$$\mathbf{Q}(t) \cdot \mathbf{A}(t) = 0; \quad \text{and} \quad \mathbf{Q}(t) \cdot \mathbf{C}(t) = 0; \quad (3)$$

because of the incompressibility condition of velocity field. This also leads to the constancy of phase of the wave i.e., $\mathbf{Q}(t) \cdot \mathbf{X} = \mathbf{q} \cdot \mathbf{x}_0$, where \mathbf{x}_0 is initial position of the fluid particle. Because of this, we can easily integrate (either numerically or analytically) the Eq. (2) to obtain the Lagrangian trajectory of the fluid particle, later to be used in the Cauchy’s solution given in Eq. (17), which is an integral equation. Such single scale flows are used in many studies exploring the intermittency, small-scale and large-scale dynamos (Gilbert & Bayly 1992; Bhat & Subramanian 2015; Kolekar, Subramanian & Sridhar 2012). One of the advantages of such a procedure is that it bypasses the closure schemes which are somewhat limiting the mean-field dynamo theories.

2.1.1 Shearing waves

When we substitute Eq. (2) in Eq. (1), the non linear term $(\mathbf{u} \cdot \nabla) \mathbf{u}$ vanishes, whereas the term $S X_1 (\partial \mathbf{u} / \partial X_2)$ is nonzero describing the interaction of large scale motion (background shear) with the turbulent velocity field \mathbf{u} . Therefore, we get time-dependent wave vectors and amplitude modulation by shear in the helical wave as shown in Eq. (2). We adopt the following expression for the velocity amplitudes (\mathbf{A}, \mathbf{C}) which were derived in Singh & Sridhar (2017):

$$[A_1(\mathbf{q}, t), C_1(\mathbf{q}, t)] = \frac{q^2}{Q^2(t)} [a_1, c_1], \quad (4)$$

$$[A_2(\mathbf{q}, t), C_2(\mathbf{q}, t)] = [a_2, c_2] + \frac{q^2}{q_{\perp}^2} \left(\frac{q_3^2}{q_2 q_{\perp}} \mathcal{M}(\mathbf{q}, t) - q_2 \mathcal{N}(\mathbf{q}, t) \right) [a_1, c_1], \quad (5)$$

$$[A_3(\mathbf{q}, t), C_3(\mathbf{q}, t)] = [a_3, c_3] - \frac{q^2 q_3}{q_{\perp}^2} \left(\frac{\mathcal{M}(\mathbf{q}, t)}{q_{\perp}} + \mathcal{N}(\mathbf{q}, t) \right) [a_1, c_1], \quad (6)$$

where

$$\mathcal{M}(\mathbf{q}, t) = \arctan \left(\frac{Q_1(t)}{q_{\perp}} \right) - \arctan \left(\frac{q_1}{q_{\perp}} \right) \quad \text{and} \quad \mathcal{N}(\mathbf{q}, t) = \frac{Q_1(t)}{Q^2(t)} - \frac{q_1}{q^2}$$

where (\mathbf{a}, \mathbf{c}) are amplitudes of the velocity field at initial time t_0 . The vectors $(\mathbf{q}, \mathbf{a}, \mathbf{c})$ form an orthogonal triad. The time-dependent wave vector is given by

$$Q^2(t) = Q_1^2(t) + q_{\perp}^2; \quad Q_1(t) = q_1 - S(t - t_0)q_2, \quad q_{\perp}^2 = q_2^2 + q_3^2. \quad (7)$$

These solutions represent the local disturbance of the velocity field in shear flows. The amplitudes (A_1, C_1) decrease with time, whereas (A_2, C_2) and (A_3, C_3) increase with time and then saturate. These helical–sheared waves rotate towards X_1 -direction (or negative X_1 -direction, depending on the initial value of \mathbf{q}) in the $X_1 - X_2$ plane as they propagate, due to the dependency of wave vector component Q_1 on shear (see, Singh & Sridhar 2017, for details).

The helicity H of the turbulent velocity field is defined as (following KSS12),

$$H = h \mathbf{C}(t) \cdot (\mathbf{Q}(t) \times \mathbf{A}(t)), \quad (8)$$

The parameter h takes values in the range $[-1, 1]$ and it controls the strength of the helicity; $h = \pm 1$ corresponds to

maximally helical flow. From the amplitudes given in Eqs. (4)–(6), it can be shown after straightforward and tedious algebra that $H = h \mathbf{c} \cdot (\mathbf{q} \times \mathbf{a})$. Even though the amplitudes $\mathbf{A}(St, \mathbf{q})$ and $\mathbf{C}(St, \mathbf{q})$ are function of shear S , helicity H of the fluid particle in this flow is independent of shear S , which is rather intriguing.

Let us construct the random flows using shearing waves, that we just introduced. In the renovating flow model, time is split into the equal intervals of length τ . The time τ is defined as the renovation time of the random process $\mathbf{u}(\mathbf{X}, t)$. The velocity field over these intervals are assumed to be distributed randomly and independently. The statistical distribution of random flow is assumed to be invariant to the shift of shearing coordinate \mathbf{x} , a natural symmetry of shear flows (Singh & Sridhar 2011). These distributions are also assumed to be constant over the intervals $[(n-1)\tau, n\tau]$; $n = 1, 2, 3, \dots$. Such ensembles simplify the dynamo problem considerably (Kraichnan 1976b; Krause & Rädler 1980). These velocity fields are stationary over the discrete times $\tau, 2\tau, 3\tau, \dots$. Hence, these can be approximated as a stationary random process over a long time ($\gg \tau$) with exponentially decaying time correlations (Molchanov et al. 1984). It is known that such velocity field together with ensemble can give rise to fast dynamo action (Finn & Ott 1988; Molchanov et al. 1985).

We employ the same ensemble as in GB92, KSS12: where Ψ is randomly distributed from 0 to 2π , this preserves the homogeneity in the shearing co-ordinates², whereas in the absence of shear, it would give usual homogeneity condition; the direction of wave vector \mathbf{q} is distributed randomly over the sphere of radius q , and this is assumed to take random direction in the successive intervals; \mathbf{a} and \mathbf{c} are distributed over the circle of radius a , perpendicular to the wave vector \mathbf{q} . At the beginning of every time interval, the wave vector \mathbf{Q} , and the amplitudes (\mathbf{A}, \mathbf{C}) are reset to it's initial values.

2.2 Evolution of mean-magnetic fields in renovating flows

The evolution of the magnetic field in the background shear flow with the velocity field $\mathbf{U}(\mathbf{X}, t) = SX_1 \mathbf{e}_2 + \mathbf{u}(\mathbf{X}, t)$ is given by

$$\left(\frac{\partial}{\partial t} + SX_1 \frac{\partial}{\partial X_2} \right) \mathbf{B} + (\mathbf{u} \cdot \nabla) \mathbf{B} - S B_1 \mathbf{e}_2 = (\mathbf{B} \cdot \nabla) \mathbf{u} + \eta \nabla^2 \mathbf{B} \quad (9)$$

As our interest is in the mean-magnetic field whose scale is much larger than the energy injection scale of turbulence, we safely ignore the diffusion term in Eq. (9), in this work. We note, however, that this would eliminate the threshold for the small-scale dynamo (SSD) in a kinematic study like this, and would lead to the growth of smaller scale magnetic structures; see, e.g., Molchanov et al. (1985); Du & Ott (1993) to also note that the growth rate of SSD is independent of microscopic resistivity as $\eta \rightarrow 0$. Thus, while magnetic fields are expected to be produced at small scales in each realization of the ensemble, these small-scale structures would average to zero in the ensemble average, by definition, which we adopt here to study only the mean magnetic field. Henceforth, we focus only on the evolution of the first moment of the magnetic field; the second moment which will be suitable for studying the SSD will be explored elsewhere.

Equation (9) is inhomogeneous in the co-ordinate X_1 , therefore, it can be best solved in shearing co-ordinates (Sridhar & Singh 2010). The shearing transformation is obtained by solving

$$\frac{d\mathbf{X}}{dt} = SX_1 \mathbf{e}_2, \quad (10)$$

which gives,

$$X_1 = x_1; \quad X_2 = x_2 + S(t - t_0)x_1; \quad X_3 = x_3, \quad (11)$$

where \mathbf{x} is the Lagrangian coordinate of fluid element carried along by the background shear flow, and t_0 is the initial time. We can write the above transformation in compact form, if we introduce $\gamma_{ij} = \delta_{ij} + S(t - t_0)\delta_{i2}\delta_{j1}$. Then, we can write Eq. (11) as

$$X_i = \gamma_{ij}(t - t_0) x_j \quad (12)$$

Let us write Eq. (9) in this new Lagrangian coordinates \mathbf{x} and time $s = t - t_0$. Also, let us introduce new vector functions for the magnetic field, $\mathbf{H}(\mathbf{x}, s) = \mathbf{B}(\mathbf{X}, t)$ and for the velocity field, $\mathbf{v}(\mathbf{x}, s) = \mathbf{u}(\mathbf{X}, t)$. Then Eq. (9) becomes,

$$\frac{\partial \mathbf{H}}{\partial s} + (\mathbf{v} \cdot \nabla) \mathbf{H} - S H_1 \mathbf{e}_2 = (\mathbf{H} \cdot \nabla) \mathbf{v}, \quad \text{with } \nabla \cdot \mathbf{v} = 0, \quad \nabla \cdot \mathbf{B} = 0, \quad (13)$$

$$\text{where } \nabla = \frac{\partial}{\partial \mathbf{x}} - S s \mathbf{e}_1 \frac{\partial}{\partial x_2} \text{ is a time dependent operator.}$$

Equation (13) differs by the original induction equation by the term $-S H_1 \mathbf{e}_2$. We can eliminate this term by transforming to a new magnetic field variable h_j which is defined from $H_i = \gamma_{ij}(s) h_j$ (similar to transformation given in Eq. (12)). Then

² The velocity correlator are independent to the shift of the shearing coordinate \mathbf{x} : $\langle \mathbf{v}_i(\mathbf{X}, t) \mathbf{v}_j(\mathbf{Y}, t') \rangle = f_{ij}(\mathbf{Q}(t) \cdot \mathbf{X} - \mathbf{Q}(t') \cdot \mathbf{Y}) = f_{ij}[\mathbf{q} \cdot (\mathbf{x} - \mathbf{y})]$, where f_{ij} 's are some function.

we can write Eq. (13) in component form as:

$$\left(\frac{\partial}{\partial s} + [\gamma_{jk}(-s)v_k] \frac{\partial}{\partial x_j} \right) h_i = h_k \frac{\partial}{\partial x_k} [\gamma_{ij}(-s)v_j] \quad (14)$$

Here we have used the property $\gamma_{ij}(s)\gamma_{jk}(-s) = \delta_{ik}$. Equation (14) is similar to the induction equation except for the velocity field, where we have obtained in its place, the transformed velocity field $v_j - Ss\delta_{j2}v_1$. We can then write the Cauchy's solution to Eq. (14) (Lundquist 1951) as,

$$h_i(\mathbf{x}, s) = \mathcal{J}_{ij}(\mathbf{x}, s)h_j(\mathbf{x}_0, 0) \quad (15)$$

where $\mathbf{x} = \mathbf{x}_0 + \int_0^s (\mathbf{v} - Ss'\mathbf{e}_2v_1)ds'$ and

$$\mathcal{J}_{ij} = \frac{\partial x_i}{\partial x_{0j}} = \delta_{ij} + \int_0^s \left(\frac{\partial v_i}{\partial x_{0j}} - Ss'\delta_{i2} \frac{\partial v_1}{\partial x_{0j}} \right) ds'. \quad (16)$$

Here \mathbf{x}_0 is the initial position of the particle at time $t = t_0$. The magnetic field H_i in the shearing frame:

$$H_i(\mathbf{x}, t) = \gamma_{ij}(t - t_0)\mathcal{J}_{jk}(\mathbf{x}_0, t - t_0)H_k(\mathbf{x}_0, t_0) \quad (17)$$

Since velocity fields are assumed to be uncorrelated on the successive intervals of the renovating flow model, we can write the evolution of magnetic field in the general interval $[(n-1)\tau, n\tau]$ as,

$$H_i(\mathbf{x}, n\tau) = \gamma_{ij}(\tau)\mathcal{J}_{jk}(\mathbf{x}_0, \tau)H_k(\mathbf{x}_0, (n-1)\tau) \quad (18)$$

We would now wish to calculate the response tensor for the average magnetic field. Since, we assume, the sheared renewing flow is homogeneous in the shearing coordinate \mathbf{x} , which is a natural symmetry in shear flows (see, Singh & Sridhar 2011), we can define the Fourier transform for the average of magnetic field $\langle H_i(\mathbf{x}, n\tau) \rangle$ in terms of the shearing waves as

$$\tilde{H}_i(\mathbf{k}, t) = \int \langle H_i(\mathbf{x}, t) \rangle \exp(-i\mathbf{k} \cdot \mathbf{x}) d^3x \quad (19)$$

where $\mathbf{k} = \mathbf{K}(t_0)$ is the initial wavevector at time t_0 , which for each interval we take to be the time $(n-1)\tau$. Here the phase of the Fourier mode is conserved in time i.e., $\mathbf{k} \cdot \mathbf{x} = \mathbf{K}(t) \cdot \mathbf{X}$, where we take t to be the time $n\tau$. Therefore, the relation between $\mathbf{K}(t_0)$ and $\mathbf{K}(t)$ is given by $k_i = \gamma_{ji}(t - t_0)K_j$ (see Sridhar & Singh (2010); Singh & Sridhar (2011) for details). We can see that the wavevectors depends on the interval of choice, which is the important distinction as compared to the case when the shear is absent, where wavevectors are time-independent. Substituting the Eq. (18) in Eq. (19), we get

$$\tilde{H}_i(\mathbf{k}, n\tau) = \int \left\langle \gamma_{ij}(\tau)\mathcal{J}_{jk}(\mathbf{x}_0, \tau) \overline{H_k(\mathbf{x}_0, (n-1)\tau)} \right\rangle_{\mathbf{x}} \exp(-i\mathbf{k} \cdot \mathbf{x}) d^3x \quad (20)$$

Since we are in the kinematic regime, where the strength of initial magnetic field is assumed weak, there is no back reaction on the velocity field (no Lorentz force). In such a scenario, the velocity field statistics become independent of the statistics of the initial magnetic field. In the following, we carry averaging in two steps: first it is performed over the initial randomness of the magnetic field, which we denoted here by over-bar in Eq. (20); and second, it is carried over the statistical ensemble of the velocity field denoted by angle-brackets. This averaging is equivalent to averaging over the energy injecting scale of turbulence q and it would introduce the effective turbulent diffusivity and smoothen the field over the scale q (Hoyng 1987). Hence, small scale magnetic structures would vanish after the ensemble average and if there is any large scale structure, it would reveal itself as a mean-field. The notation $\langle \rangle_{\mathbf{x}}$ indicate that the averaging is carried over that trajectory, in each realization, which reaches a fixed point \mathbf{x} at time $n\tau$. By homogeneity of velocity field statistics in the shearing coordinate \mathbf{x} , the averaging becomes independent of spatial point \mathbf{x} . The initial magnetic field need not be homogeneous and its spatial dependency can be taken into account by the Fourier transform as defined by Eq. (19). Thus, using all the ingredients, we obtain³

$$\tilde{H}_i(\mathbf{k}, n\tau) = \mathcal{G}_{ik}(\mathbf{k}, \tau)\tilde{H}_k(\mathbf{k}, (n-1)\tau), \quad (21)$$

where

$$\mathcal{G}_{ik}(\mathbf{k}, \tau) = \left\langle \gamma_{ij}(\tau)\mathcal{J}_{jk}(\mathbf{x}_0, \tau) e^{-i\mathbf{k} \cdot (\mathbf{x}_0 - \mathbf{x})} \right\rangle \quad (22)$$

Here, $\mathbf{k} = \mathbf{K}[(n-1)\tau]$ as defined before. Here, we have $K_i(n\tau) = \gamma_{ji}(-\tau)K_j[(n-1)\tau]$. Thus, we can note that K at $(n-1)\tau$ is related to the wavevector at $n\tau$ by inverse shearing transformation described in Eq. (11). Note here that, the response tensor \mathcal{G}_{ij} depends on the time-step $(n-1)\tau$ through \mathbf{K} , where \mathbf{K} is continuously sheared till the time $(n-1)\tau$. Since, we have neglected diffusion term in the induction equation, we will always have the growth of the magnetic field $\mathbf{H}(\mathbf{x}, t)$ in a single realization of the ensemble. However, to know the growth at large scale, we have defined the ensemble averaged

³ The mean-magnetic field in Fourier space at mode \mathbf{k} has contribution only from the initial magnetic field at mode \mathbf{k} , which is an important simplification that is occurred, because of the homogeneity condition in the shearing coordinate \mathbf{x} .

mean-field $\langle \mathbf{H}(\mathbf{x}, t) \rangle$, which may or may not grow. For example, if $h = 0$, the mean-field $\langle \mathbf{H}(\mathbf{x}, t) \rangle$ will decay (see subsection 2.4), whereas $\mathbf{H}(\mathbf{x}, t)$ might grow at small scales due to SSD. Here, we are only concerned with the growth of mean magnetic field, or the first moment.

2.3 Growth rate and cycle periods of the magnetic field

We can say, a given velocity field will lead to dynamo, if there is an exponential growth of magnetic field in time (Dittrich et al. 1984; Molchanov et al. 1984). In the renovating flow, we are interested in the behaviour of the magnetic field at longer times i.e., as $n \rightarrow \infty$. Because, the flow is stationary in the discrete translation of times $n\tau$, $n = 1, 2, 3, \dots$, we can consider velocity field as stationary for long times ($n\tau \gg \tau$). Hence, it became possible to construct the eigenvalue problem in any interval $[(n-1)\tau, n\tau]$ for the evolution of the mean-magnetic field (see Eq. (21)) in previous subsection. The magnetic field will grow, if the magnitude of the leading-complex-eigenvalue of the response tensor (given in Eq. (22)) is greater than unity. And the final magnetic field will be the eigenvector of response tensor corresponding to that leading eigenvalue, irrespective of the magnitude and direction of the initial magnetic field. If σ is the leading eigenvalue, we can define the exponential ($\exp(\lambda t)$) growing exponent λ as,

$$\lambda = \frac{1}{\tau} \ln \sigma(\mathbf{k}, \tau) = \frac{1}{\tau} \ln |\sigma| + i \frac{\arg(\sigma)}{\tau} \quad (23)$$

Since, the response tensor depends on the interval in which magnetic field growth is considered, eigenvalues will also depend on the corresponding interval through $\mathbf{k} = \mathbf{K}[(n-1)\tau]$. This will lead to the important conclusion i.e., non-axisymmetric modes will decay eventually, which will be elucidated in Section 3. The real part will define the growth rate of the magnetic field, whereas the imaginary part will define frequency of the wave, which will be used to calculate the cycle period of the dynamo wave. Below, we give expressions for both,

$$\gamma = \frac{1}{\tau} \ln |\sigma|, \quad P_{\text{cyc}} = \frac{2\pi\tau}{\arg(\sigma)} \quad (24)$$

where $\arg(\sigma) = 0$ represent the standing wave and $\arg(\sigma) \neq 0$ indicate the travelling dynamo wave.

2.4 Method of averaging

To compute the Green's tensor given in Eq. (22), we need to obtain the Jacobian of transformation between fluid particle at position \mathbf{x} at $n\tau$ with the initial position \mathbf{x}_0 at time $(n-1)\tau$. For general velocity field, we need to solve for \mathbf{x} from the equation $d\mathbf{x}/dt = \mathbf{v}(\mathbf{x}, t)$, which itself is a formidable task. Since, the velocity field considered in Eq. (2) has constancy of phase ($\mathbf{Q} \cdot \mathbf{X} = \mathbf{q} \cdot \mathbf{x}_0$) due to the incompressibility condition ($\nabla \cdot \mathbf{v} = 0$), we can integrate the velocity field to obtain the Jacobian of the transformation as

$$\mathcal{J}_{ij} = \frac{\partial x_i}{\partial x_{0j}} = \delta_{ij} + q_j [\tilde{a}_i(t, \mathbf{q}) \cos(\mathbf{q} \cdot \mathbf{x}_0 + \psi) - h \tilde{c}_i(t, \mathbf{q}) \sin(\mathbf{q} \cdot \mathbf{x}_0 + \psi)] \quad (25)$$

where

$$\tilde{a}(t, \mathbf{q}) = \int_{(n-1)\tau}^{n\tau} [\mathbf{A} - S(t-t_0)A_1 \mathbf{e}_2] dt \quad (26)$$

$$\tilde{c}(t, \mathbf{q}) = \int_{(n-1)\tau}^{n\tau} [\mathbf{C} - S(t-t_0)C_1 \mathbf{e}_2] dt \quad (27)$$

Here $t_0 = (n-1)\tau$. We can easily average the Green's tensor in Eq. (22) over the phase Ψ (see KSS12 for details) to get,

$$G_{ij}(\mathbf{k}) = \gamma_{ik}(\tau) \left\langle \delta_{kj} J_0(\Delta) - ih \frac{q_j [\mathbf{k} \times (\tilde{\mathbf{a}} \times \tilde{\mathbf{c}})]_k}{\Delta} J_1(\Delta) \right\rangle_{\mathbf{q}, \mathbf{a}} \quad (28)$$

where $\Delta = \sqrt{(\mathbf{k} \cdot \tilde{\mathbf{a}})^2 + h^2 (\mathbf{k} \cdot \tilde{\mathbf{c}})^2}$ and, J_0 and J_1 are Bessel functions of order zero and one, respectively. Because, we have $J_0(y) \leq 1, \forall y$, the term that is relevant for the dynamo action would be the second term in Eq. (28) containing the parameter h , which characterizes the kinetic helicity. When $h = 0$, i.e., strictly non helical case, there is no mean-field dynamo as already pointed out in KSS12. We have chosen $h = 1$, which corresponds to maximally helical flow, throughout this work.

We perform remaining averages—over $(\mathbf{q}, \mathbf{a}, \mathbf{c})$ —numerically. We know that, \mathbf{q} , \mathbf{a} and \mathbf{c} vectors form orthogonal triad. Using the three Euler angles for the rigid body rotation, we can relate the triad $(\mathbf{q}, \mathbf{a}, \mathbf{c})$ to the direction of magnetic field wave vector (k_1, k_2, k_3) at time equal zero. We use Gauss quadrature methods to perform all the integrals. Further details will be given in the next paper II, which focus on the role of helicity fluctuations on the growth of mean magnetic field. We numerically

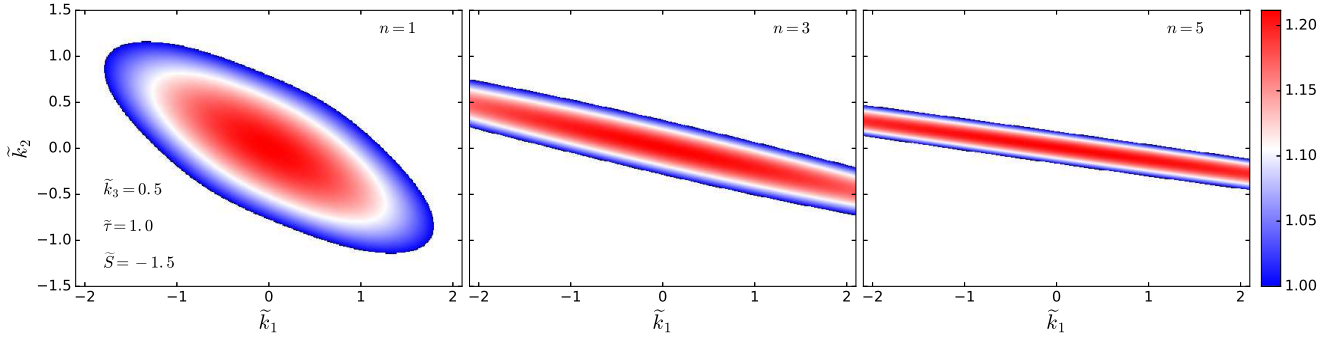


Figure 1. Contours of the magnitude of leading eigenvalue σ in $k_1 - k_2$ at $k_3 = 0.5$, obtained at the end of first (left), third (middle) and fifth (right) interval n ; time increases from left to right as $n = t/\tau$.

determine the eigenvalues of the response tensor $\hat{\mathcal{G}}$ which governs the evolution of mean magnetic field. The growth rate and cycle period can then be obtained from Eq. 24. Below we discuss the non-axisymmetric and axisymmetric mean field dynamos. We present our findings in the non-dimensional units, henceforth. All the quantities are suitably normalized with respect to eddy turn-over time of the flow at the beginning of each interval, $T = 1/qa$, and the wave vector q . Quantities with over-tilde are made dimensionless in this way, e.g., $\tilde{\mathbf{k}} = \mathbf{k}/q$, $\tilde{\gamma} = \gamma T$, $\tilde{\alpha}_{ij} = \alpha_{ij}/a$, and so on.

3 DECAY OF NON-AXISYMMETRIC MODES OF MEAN MAGNETIC FIELD

We show in this subsection that the non-axisymmetric mode of the mean-magnetic field decays asymptotically. Since shearing flows are anisotropic in all three directions, the eigenvalues of the response tensor for the magnetic field will also be anisotropic in the directions of k_1 , k_2 and k_3 . We have decomposed the magnetic field in the shearing waves (see Eq. (19)), where we have used time dependent wave vector. If (k_1, k_2, k_3) be the wave vector of the magnetic field at time $t = 0$, then at $t = n\tau$, it would become $(k_1 - n S\tau k_2, k_2, k_3)$.

Let us denote the magnetic field by the column vector \hat{H} and response tensor by the square matrix $\hat{\mathcal{G}}$ (see Eq. (21)). Let \hat{H}_0 be the initial magnetic field at $t = 0$, then the magnetic field at $t = n\tau$ is given by

$$\hat{H}_n = \hat{\mathcal{G}}_n \dots \hat{\mathcal{G}}_2 \hat{\mathcal{G}}_1 \hat{H}_0 \quad (29)$$

where $\hat{\mathcal{G}}_n$ indicate the response tensor in n^{th} interval with sheared wavevector $(k_1 - n S\tau k_2, k_2, k_3)$.

We now describe the procedure to determine \hat{H}_n iteratively. At the end of the first interval, we get $\hat{H}_1 = \hat{\mathcal{G}}_1 \hat{H}_0$. We find that one of the eigenvectors of $\hat{\mathcal{G}}_1$ does not satisfy $\mathbf{k} \cdot \mathbf{H}_0 = 0$. Let \hat{V}_{01} and \hat{V}_{02} be the eigenvectors (with corresponding eigenvalues being σ_{01} and σ_{02}), such that, they are orthogonal to the direction of \mathbf{k} . We can now express the initial magnetic field in terms of the eigenvectors as

$$\hat{H}_0 = C_{01} \hat{V}_{01} + C_{02} \hat{V}_{02} \quad (30)$$

where C_{01} and C_{02} are some complex constants. The quantity \hat{H}_1 thus becomes:

$$\hat{H}_1 = C_{01} \sigma_{01} \hat{V}_{01} + C_{02} \sigma_{02} \hat{V}_{02} \quad (31)$$

For the next iteration, that is at $t = 2\tau$, we have $\hat{H}_2 = \hat{\mathcal{G}}_2 \hat{H}_1$. The response tensor $\hat{\mathcal{G}}_2$ is modified because the magnetic field wave vector (k_1, k_2, k_3) would shear to $(k_1 - S\tau k_2, k_2, k_3)$. Hence, \hat{V}_{01} and \hat{V}_{02} will not anymore be the eigenvectors of $\hat{\mathcal{G}}_2$. We need to express the eigenvectors \hat{V}_{01} and \hat{V}_{02} in terms of the eigenvectors of $\hat{\mathcal{G}}_2$. Similarly, let \hat{V}_{11} and \hat{V}_{12} be the eigenvectors (with corresponding eigenvalues being σ_{11} and σ_{12}) of the response tensor $\hat{\mathcal{G}}_2$ orthogonal to the direction of $(k_1 - S\tau k_2, k_2, k_3)$. Then we have,

$$\hat{V}_{01} = C_{11}^{(1)} \hat{V}_{11} + C_{12}^{(1)} \hat{V}_{12} \quad \hat{V}_{02} = C_{11}^{(2)} \hat{V}_{11} + C_{12}^{(2)} \hat{V}_{12} \quad (32)$$

where $C_{11}^{(1)}$, $C_{12}^{(1)}$, $C_{11}^{(2)}$ and $C_{12}^{(2)}$ are again some complex constants.⁴ Using Eq. (32) in Eq. (31), we get

$$\hat{H}_2 = (\dots \sigma_{01} \sigma_{11} + \dots \sigma_{02} \sigma_{11}) \hat{V}_{11} + (\dots \sigma_{01} \sigma_{12} + \dots \sigma_{02} \sigma_{12}) \hat{V}_{12} \quad (33)$$

⁴ Note here that, we have suppressed the third component of \hat{V}_{01} and \hat{V}_{02} . Because at every interval we need to satisfy the solenoidality condition ($\nabla \cdot \mathbf{H} = 0$).

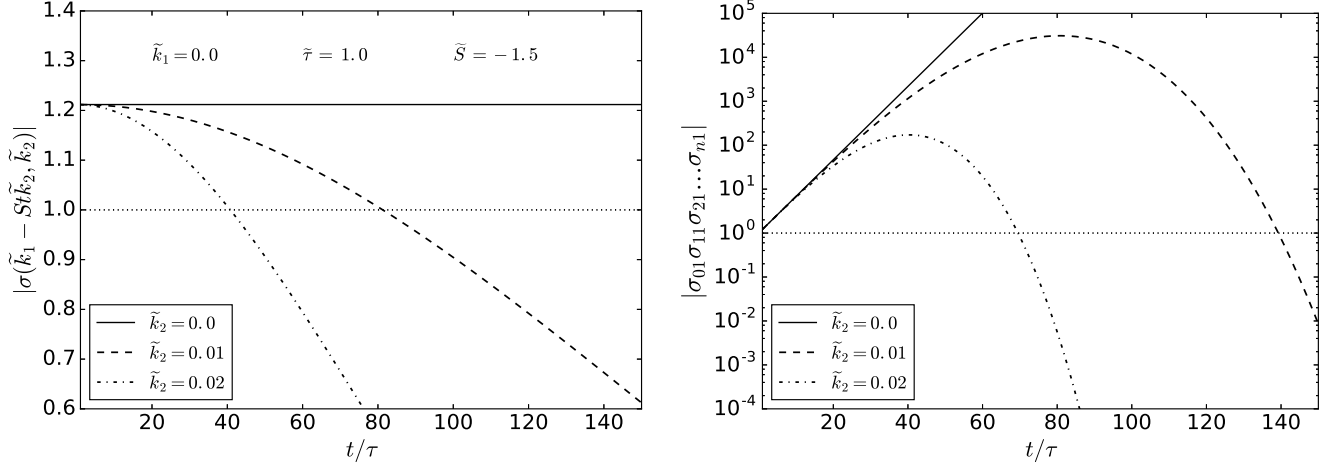


Figure 2. (Left) Magnitude of the leading eigenvalue and (right) cumulative product of the maximum eigenvalues as a function of $n = t/\tau$, i.e., the interval of the renovating flow.

where ellipsis indicate pre-multiplied factors, such as multiplication of complex coefficients. As we continue to iterate in the above manner by expressing the preceding eigenvectors in terms of the current eigenvectors (like in Eq. (32)), we get 2^{n+1} terms for the magnetic field \hat{H}_n at the end of n^{th} interval; at every interval, the number of terms are doubled. Of the two relevant eigenvectors at any interval, let us say that we have, $|\sigma_{n1}| > |\sigma_{n2}|$, then in those 2^{n+1} terms, there will be a term of the kind $\sigma_{01}\sigma_{11}\sigma_{21}\dots\sigma_{n1}$ whose magnitude will be the largest compared to other terms. To demonstrate that non-axisymmetric modes decay eventually, it is enough to show that this term decays after some interval of time.

In Figure 1 we have shown the magnitude of the largest eigenvalues σ_{n1} in the $k_1 - k_2$ plane for $k_3 = 0.5$ at the end of first ($t = \tau$), third ($t = 3\tau$), and fifth ($t = 5\tau$) interval. We have highlighted the area where $|\sigma_{n1}| > 1$, which represents the transient growth region. As time is increasing, the wave vector is continuously sheared in the k_1 direction, the transient growth region is stretched in the k_1 direction, and it diminishes in the k_2 direction. As time continues, the growth region aligns with the $k_2 = 0$ axis, and eventually vanishes. To make this point clear, let us consider the wavevectors, which lie close to maxima of the contours shown in Figure 1, i.e., $(0,0)$ in $k_1 - k_2$ plane. In the left panel of Figure 2, we have shown the largest eigenvalue as the function of intervals for three different values of k_2 . When $k_2 = 0$ (axisymmetric mode), the magnitude of the largest eigenvalue remains constant as the wavevector $(k_1, 0, k_3)$ remains same across the intervals. Therefore the cumulative product of the magnitude of the eigenvalues $|\sigma_{01}\sigma_{11}\sigma_{21}\dots\sigma_{n1}| = |\sigma_{01}|^n$, increases monotonically leading to the exponential growth of the axisymmetric mode of the magnetic field (see Figure 2: right panel, black solid line). For $k_2 \neq 0$, the wave vectors are time dependent. As time increases, the value of $k_1 - Stk_2$ increases (for negative S), eventually the wave vector moves out of the transient growth region i.e., the region where $|\sigma_{n1}| > 1$ (see Figure 1). As shown in Figure 2 (left panel), for $k_2 = 0.01$ ($k_2 = 0.02$), the magnitude of eigenvalue falls below unity around $t = 80\tau$ ($t = 40\tau$). The magnitude of the cumulative product of the largest eigenvalues $|\sigma_{01}\sigma_{11}\sigma_{21}\dots\sigma_{n1}|$ increases for some time (see right panel in Figure 2) and then it starts to decrease, and falls below unity leading to the decay of the mode. Hence, non-axisymmetric modes will only have transient growth before decaying eventually. Even though, the analysis of this section is made with the particular velocity field, its validity remains general. Because, essential argument to show the asymptotic decay needs only two ingredients: the magnetic wave vector is time-dependent, which is a consequence of background shear flow; and the growth region is limited in the k -space, which is the consequence of the finite correlation of velocity field rather than its particular choice. Therefore, in the kinematic dynamo regime, non-axisymmetric mode have no active role to play.

4 GROWTH OF AXISYMMETRIC MODES OF MEAN MAGNETIC FIELD

From now onward we focus only on the axisymmetric solutions for which $k_2 = 0$, as the non-axisymmetric modes are expected to decay as discussed above. Since, for axisymmetric modes the eigenvalues and eigenvectors are constant in time, we just need to consider its growth rate in a single interval (see the black solid line in left panel of Figure 2). With σ being the leading eigenvalue of the response tensor, we find that the magnetic field at the end of the n^{th} interval is given by $H_n = \sigma^n H_0$ where H_0 is the initial magnetic field, also assumed to be the corresponding eigenvector. Figure 3 shows contours of normalized growth rate $\tilde{\gamma} = \gamma T$, with its positive values indicating exponentially growing solutions in k_1 - k_3 plane for axisymmetric mean field dynamos, as functions of the two parameters, the shear rate S , and the renovation time τ . Note that $T = 1/qa$ is the

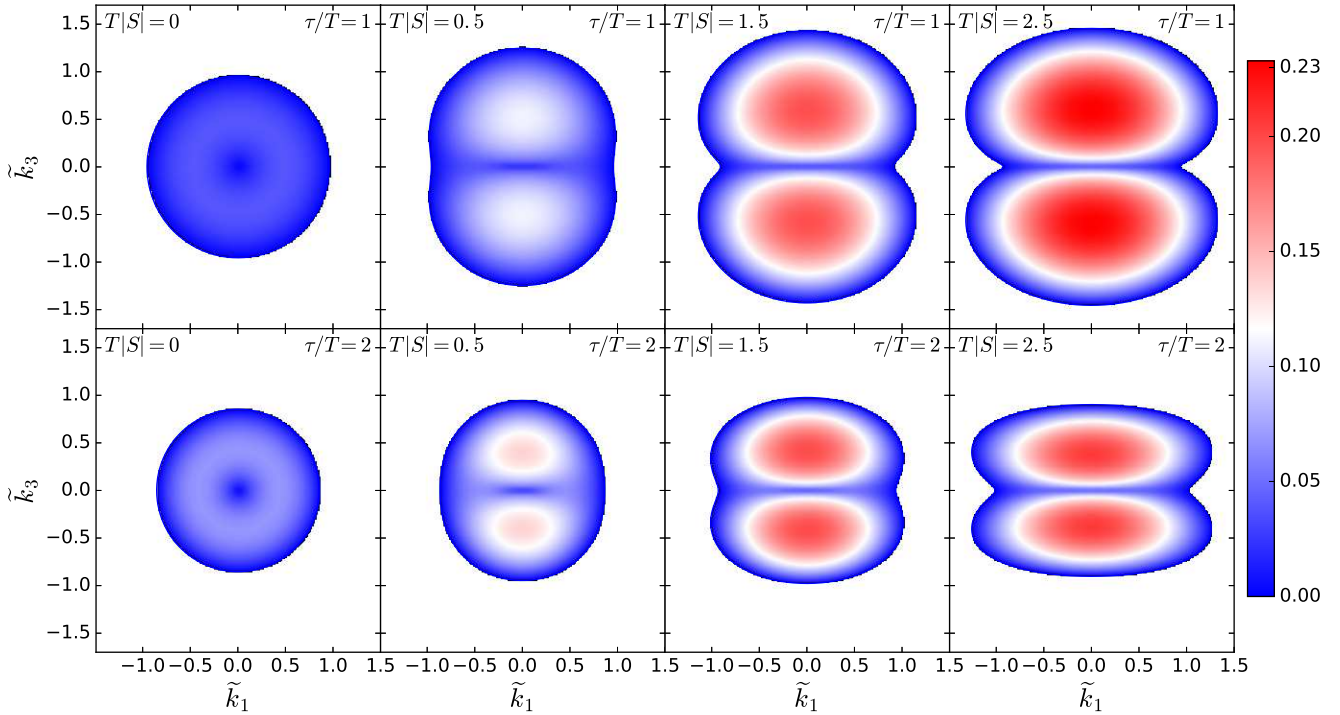


Figure 3. Contours of growth rate $\tilde{\gamma} \geq 0$ in $k_1 - k_3$ plane for axisymmetric (i.e., $k_2 = 0$) mean field dynamos. Shear increases from left to right, with $\tau/T = 1$ (top) or $\tau/T = 2$ (bottom). Regions outside the outermost (blue) contour do not support a dynamo instability.

eddy turnover time of the random helical flow at the beginning of each interval. Regions enclosed within the outermost (blue) contours in Figure 3 is referred as dynamo regions.

For zero shear, dynamo regions are circularly symmetric about the origin $k_1 = k_3 = 0$; see leftmost panels in Figure 3. The other panels there reveal that the dynamo regions gets bifurcated for non-zero shear. Note that the maximum growth occurs along k_3 axis when $k_1 = 0$. Therefore, without any loss of generality, and in order to capture the branch containing the fastest growing mode, we set $k_1 = 0$ henceforth. We also find from this figure that the growth rate is symmetric about the point $k_3 = 0$, and therefore we consider only positive values of k_3 to explore its behaviour as a function of wavenumber. Thus, we have now set $k_1 = k_2 = 0$, which is equivalent of taking average over entire X_1 - X_2 plane, i.e., the plane of background shear, and we study one dimensional mean field dynamo modes propagating along X_3 direction.

Interestingly, the wavenumber corresponding to the fastest growing mode, denoted by k_* , varies non-monotonically with the strength of shear $|S|$ when the renovation time τ , which is the same as the correlation time of the flow, becomes comparable to the eddy turnover time T . This is better shown in Figure 4, where various curves correspond to different choices of τ/T . However, when $\tau/T \ll 1$, i.e., when the memory effects are unimportant as the random flow is nearly of white-noise type, the maximum growth occurs at progressively smaller spatial scales ($\sim k_*^{-1}$) with increasing shear strengths; sufficiently strong shear produces magnetic field preferentially at scales smaller than the eddy size given by q^{-1} , i.e., $k_*/q > 1$, as may be seen from the dash dotted curve. It is only when τ/T becomes of order unity, the shear gets some time to act and it changes the scenario even qualitatively; see also Sridhar & Subramanian (2009). It promotes a genuine large-scale dynamo as $k_*/q < 1$ for a whole range of shear, i.e., in this case, the mean magnetic field grows maximally at scales larger than the eddy scale. Also note that at fixed shear, k_* systematically decreases when τ increases; see also Appendix (A) where we show a comparison with a case when non-shearing waves are used to model the renovating flow.

4.1 Growth rate

In Figure 5 we show the behaviour of normalized growth rate $\tilde{\gamma}$ of the mean magnetic field as a function of wavenumber k_3 . We have chosen two large values for the correlation time τ in the two panels, where different curves in each panel correspond to different values of shear rate S ; $\tau/T = 1$ and 2 in left and right panels, respectively. Regardless of the strength of the shear, including its zero value, the growth rate first increases from zero as a function of k_3 , attains a maximum, then it decreases to become negative at sufficiently large wavenumbers. Note again that the maximum lies at wavenumbers that are smaller than the one corresponding to random eddies, and magnetic fields at sufficiently large wavenumbers are always suppressed.

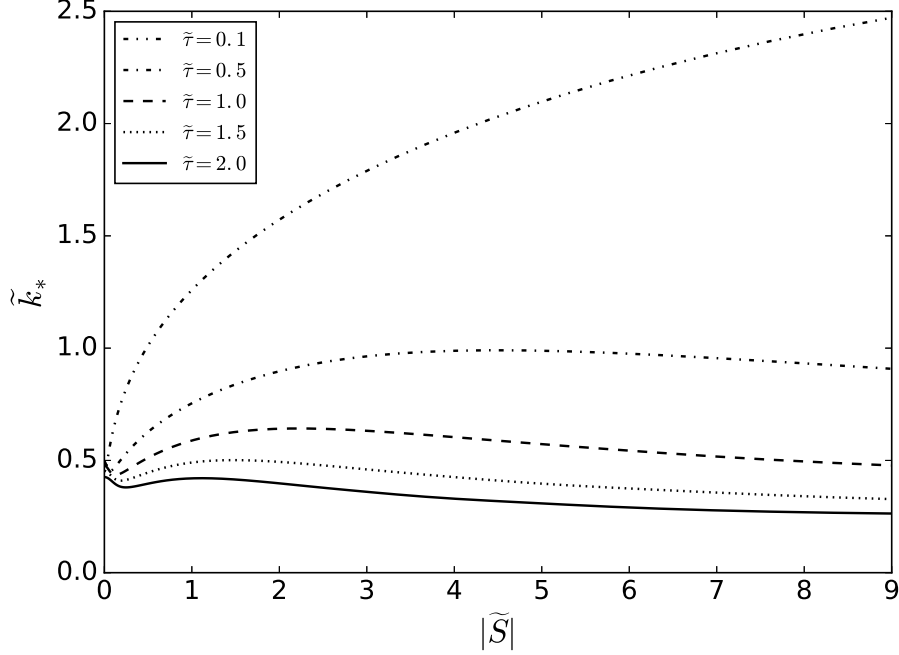


Figure 4. Dependence of k_*/q (wavenumber corresponding to the fastest growing mode) on shear for different choices of τ/T .

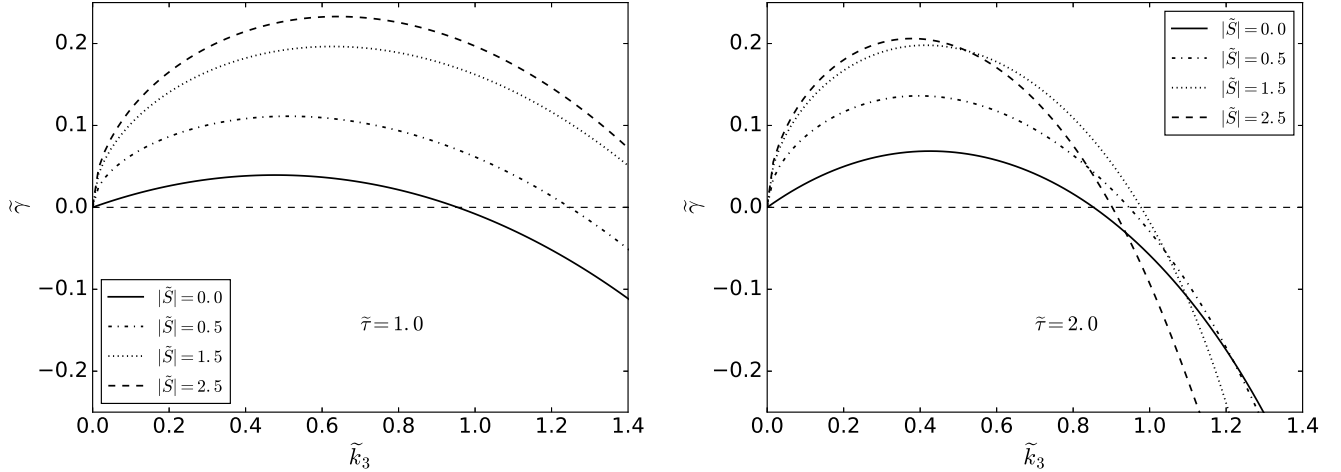


Figure 5. Normalized growth rate $\tilde{\gamma}$ as a function of wavenumber k_3 , for $\tau/T = 1$ (left) and $\tau/T = 2$ (right). Different curves in each panel correspond to different values of shear rate S .

Looking first at the more reasonable case with $\tau/T = 1$, we find that the growth rate increases at all the wavenumbers shown, when the shear parameter \tilde{S} is increased from zero to a moderately large values; see left panel of Figure 5 where $0 \leq \tilde{S} \leq 2.5$. However, the behaviour is more complicated when $\tau/T = 2$, as, at fixed $k_3 \gtrsim q$, shear leads to suppression of mean magnetic fields; see the right panel. Nevertheless, the peak of the growth rate remains at much smaller wavenumbers, thus enabling a large-scale dynamo.

Now we turn to the dependence of the growth rate of mean-field dynamo on the shear. We saw earlier in Figure 4 that the wavenumber (k_*) corresponding to the fastest growing mode is itself a function of shear. Therefore, in Figure 6, we show the shear dependence of the growth rate $\tilde{\gamma}$ at k_* . Remarkably, the growth rate shows a non-monotonic trend with the shear strength in more realistic regime when the correlation time τ of the random helical flow becomes comparable to the eddy turn over time T ; see, e.g., dotted or solid curves in Figure 6. The growth rate here is always positive, even when shear approaches zero, due to the fact that we have chosen maximally helical random flow ($h = 1$). Initially, the growth rate remains constant as shear increases, and this constant is a function of correlation time. For $\tilde{\tau} = 0.1$, we have $\tilde{\gamma} \simeq 4 \times 10^{-3}$ and for $\tilde{\tau} = 2.0$, we

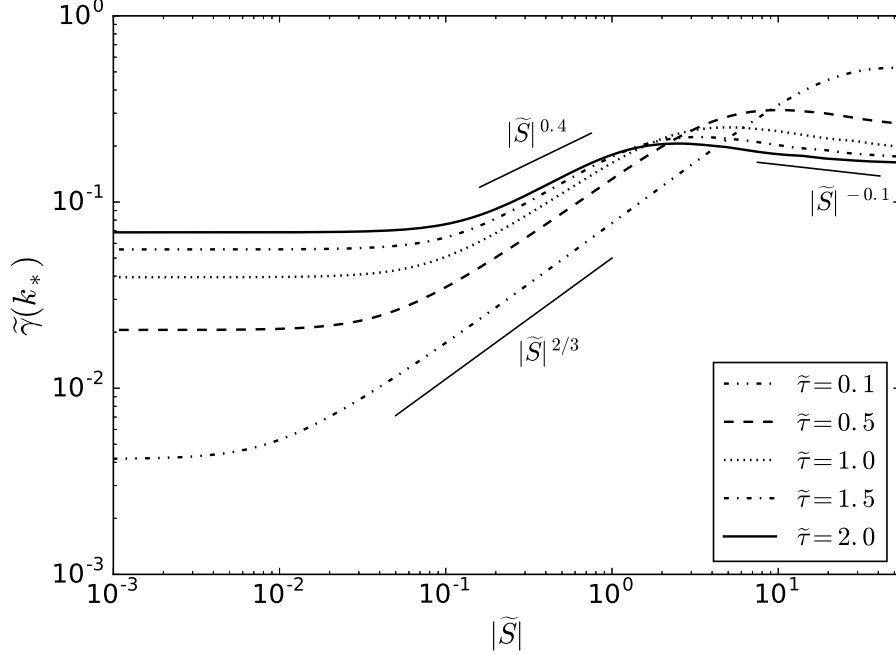


Figure 6. Growth rate of fastest growing mode as a function of shear for different choices of velocity correlations times τ .

have $\tilde{\gamma} \simeq 6,5 \times 10^{-2}$ (see Figure 6); dynamo becomes more efficient at a fixed weak shear as correlation time increases. As shear strength increases, the growth rates starts to increase, as can be seen from Figure 6. The growth rate varies as $\tilde{\gamma} \sim S^{2/3}$ for $\tilde{\tau} = 0.1$ and as $\tilde{\gamma} \sim S^{0.4}$ for $\tilde{\tau} = 2.0$, in the intermediate shear range. As the shear strength further increases, the growth rate starts to decrease as $\tilde{\gamma} \sim S^{-0.1}$ after reaching the maximum. This decrease is happening at large shear because, the transport coefficient like α_{ij} is a function of shear and decreases as the shear strength increases (see Figure 7)⁵. This results in quenching of the dynamo at strong shear. Our results are in agreement with the work of Leprovost & Kim (2008) who also reported dynamo quenching due to strong shear. Note that this is unlike more popular expectation based on standard kinematic $\alpha\Omega$ dynamos, where the dynamo efficiency increases monotonically with shear. Such expectations have resulted in common notion that the regions with strongest shear in a system, e.g. the tachocline in case of the Sun, must be the best reservoirs of magnetic fields. We envisage that the dynamo quenching being reported here in the strong shear regime will be helpful for a better understanding in this direction.

4.2 α -effect

By adapting to a standard textbook definition of α_{ij} , we make an attempt to determine the components of α tensor based on the random velocity fields we have chosen in our model. This may provide useful insights for key mechanisms that govern the properties of the large-scale dynamo action we study in this work. More precisely, it may help us understand the reason for dynamo quenching at large shear as shown earlier in Figure 6. We have chosen the following definition (see, Moffatt 1978, section 7.10):

$$\alpha_{ij}(\tau) = \frac{1}{\tau} \int_0^\tau dt \int_0^t dt' \hat{\alpha}_{ij}(t, t') \quad \text{with} \quad \hat{\alpha}_{ij}(t, t') = \epsilon_{ilk} \left\langle v_l(\mathbf{x}_0, t) \frac{\partial v_k(\mathbf{x}_0, t')}{\partial x_j} \right\rangle. \quad (34)$$

Here the velocity field \mathbf{v} is given from Eq. (2) in terms of time-dependent shearing waves with fixed helicity (Singh & Sridhar 2017). This evolves for the renovation time interval τ which represents one single realization. The average is then taken over many such realizations, or equivalently, over time $t = n\tau$ with $n \rightarrow \infty$. The second integral is taken to average the α -tensor over the interval from 0 to τ . Note that while the velocity \mathbf{v} gets randomized after every τ , the kinetic helicity associated with it stays constant for all times in the present work. Following Rädler et al. (2003) we symmetrize the α_{ij} defined in Eq. (34) as $\alpha_{ij}^S = (\alpha_{ij} + \alpha_{ji})/2$; the antisymmetric part corresponds to the turbulent pumping which we ignore in this study. In Figure 7

⁵ See also appendix (A) for the behaviours of γ and k_* , for the case when flow amplitudes are constant, i.e., independent of shear. In such a scenario, transport coefficients also become independent of shear.

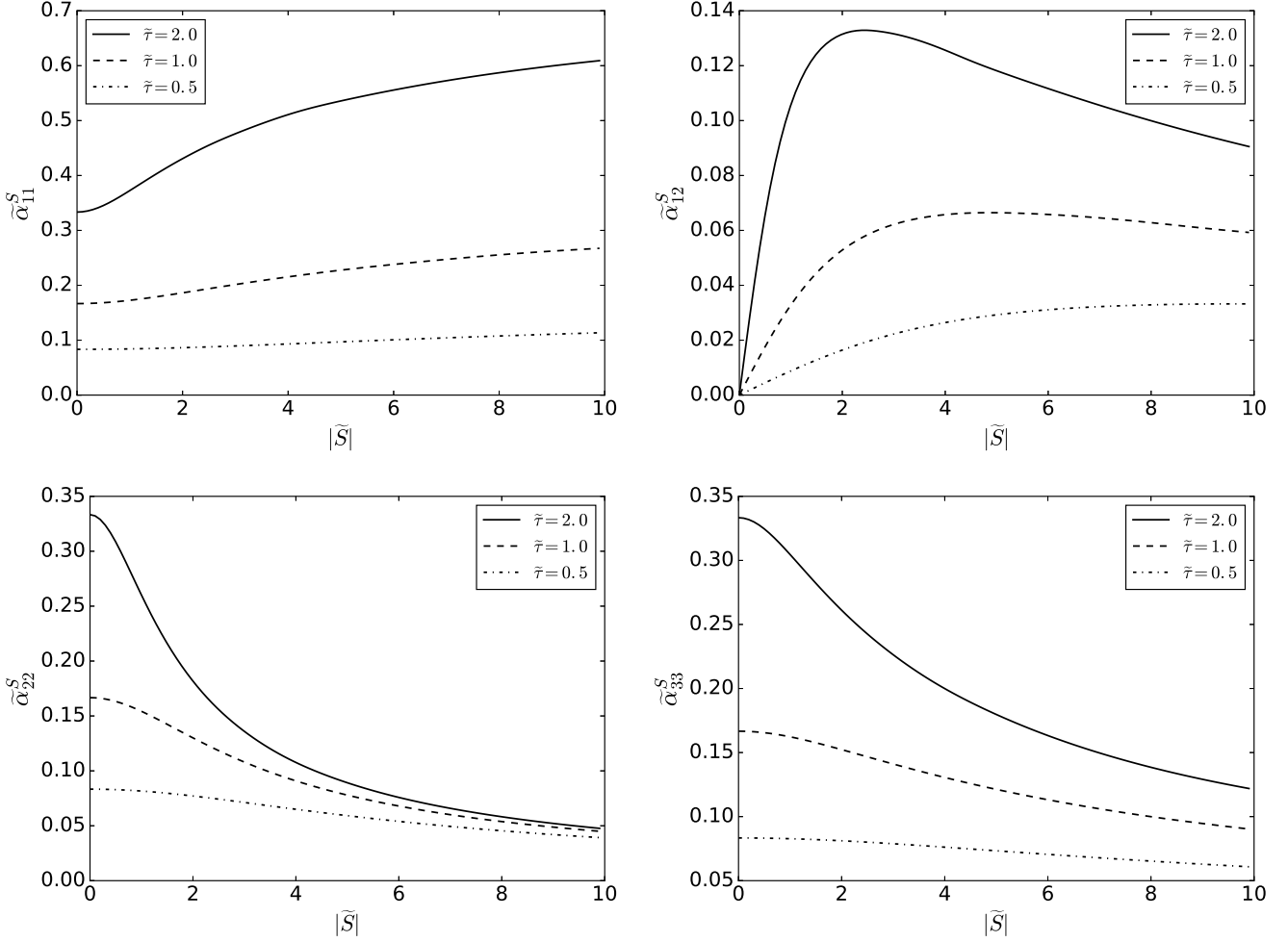


Figure 7. Behaviour of non-zero components of symmetric tensor $\tilde{\alpha}_{ij}^S$ with $|\tilde{S}|$. Different curves correspond to different choices of $\tilde{\tau}$.

we show the behaviour of non-zero components of dimensionless quantity $\tilde{\alpha}_{ij}^S$ as a function of shear; other components vanish identically for our choice of random velocity field. While α_{11} shows an increase with $|S|$, α_{22} and α_{33} are significantly quenched when shear becomes too large. The behaviour of $\tilde{\alpha}_{12}^S$ is more involved as may be seen from the Figure 7. The trace of α -tensor i.e., $\alpha_{11} + \alpha_{22} + \alpha_{33}$ is also a decreasing function of shear. Note that the helicity as defined by Eq. (8) is independent of shear rate S . Also, at a fixed value of shear, magnitudes of all the components increase with $\tilde{\tau} = \tau/T$, where we note again that τ and T represent velocity correlation and eddy turn over times, respectively. Thus, we find that the α -tensor is strongly affected by the presence of shear, with effect being more pronounced when velocity correlation times τ are comparable to the eddy turn over time T .

4.3 Cycle period of dynamo waves

Another important quantity is the cycle period of the growing dynamo wave. This is denoted by P_{cyc} and defined in Eq. (24). Its behaviour at k_* as a function of shear is shown in Figure 8. It falls with shear as $|S|^{-1}$ for all τ when shear is weak, but this scaling becomes shallower at larger values of shear rate. Interestingly enough, P_{cyc} becomes nearly independent of shear, when normalized absolute shear $|\tilde{S}| \gtrsim 1$ and $\tau/T \sim \mathcal{O}(1)$. Thus our present model yields, for a dimensionless quantity $1/(|S|P_{\text{cyc}})$ (see the inset of Figure 8), a scaling of (i) $|S|^0$, i.e., independent of shear, at weak shear, and (ii) $|S|^{-1}$ when shear becomes sufficiently strong.

Note that the standard $\alpha\Omega$ ($\alpha^2\Omega$) dynamo predicts a uniform scaling, $P_{\text{cyc}} \sim |S|^{-1/2}$ ($|S|^{-1}$), with shear. It is intriguing to note here that Olsper et al. (2018), based on their observational analysis, found evidence of two distinct population of stars, inactive and active, which reveal different scalings in a stellar magnetic activity-rotation diagram. Standard dynamo models fail to explain the existence of these branches in such a diagnostic diagram, which provides a sufficient motivation for further work on this topic of turbulent dynamo action due to helicity and shear; see Olsper et al. (2018), and references

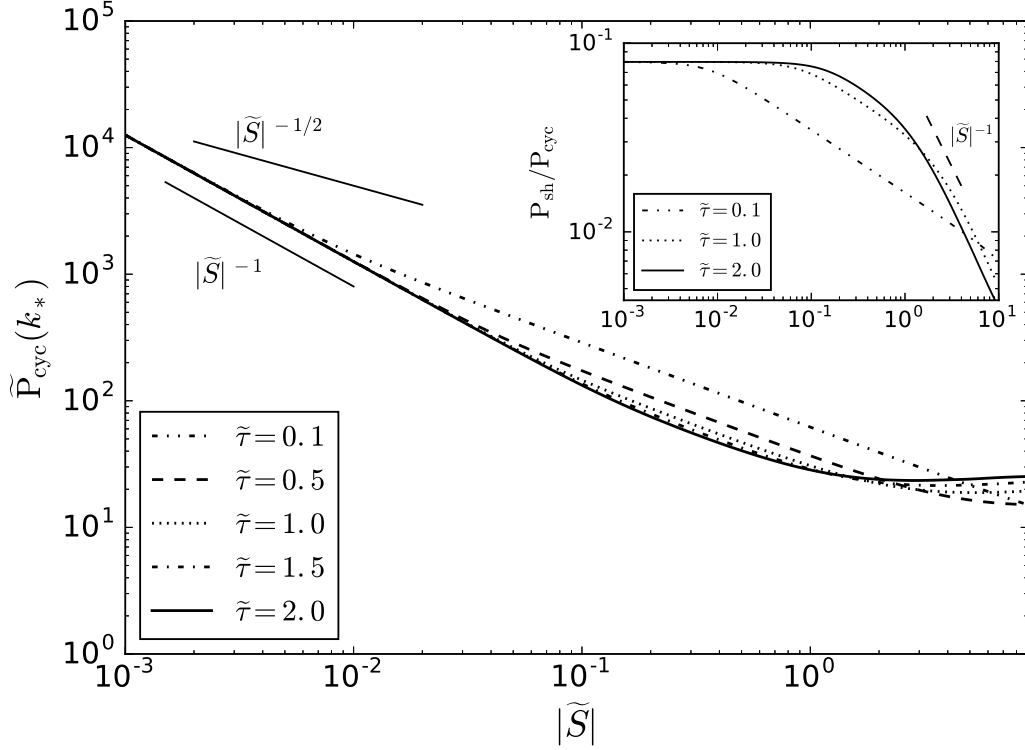


Figure 8. Cycle period of dynamo wave as a function of shear for different values of τ . Inset: Dimensionless quantity $P_{\text{sh}}/P_{\text{cyc}}$ as a function of shear, where $P_{\text{sh}} = 1/|S|$.

therein, to appreciate the importance of studying the cycle periods of dynamos, as this offers a unique opportunity to test model predictions. We believe that the new scaling laws which we find in this work will have implications for the interpretation of the observations of magnetic activity cycles seen in Olsper et al. (2018).

5 CONCLUSIONS

In this paper, we have studied the problem of generation of large-scale magnetic field due to random flows with fixed kinetic helicity and finite correlation times in a shearing background. We employed a pulsed renewing flow based model where flow field renovates itself after every time interval τ , called here the correlation time of the inviscid random helical flow. We made use of single plane shearing waves with fixed kinetic helicity to model the renovating flow. These are time-dependent exact solutions to the Navier-Stokes equations as derived by Singh & Sridhar (2017). Thus we self-consistently included the anisotropic effects of shear on the flow itself, which in turn governs the evolution of magnetic fields. We constructed the suitable ensemble of realization for the velocity field, later to be used in the averaging of magnetic field. By making a suitable use of shearing coordinate transformation, we wrote the ideal induction equation in a shearing frame which translates with the background linear shear flow. The evolution of magnetic field is determined in terms of Cauchy's solutions in a fixed interval τ which represents a single realization. Because of discrete time-translational symmetry of renovating flow in $n\tau$, we could construct the eigenvalue problem for the mean magnetic field in Fourier space in any interval. The Green's function or the propagator (or simply average response tensor), which maps the mean-field at $(n-1)\tau$ to $n\tau$ is obtained after performing an average over many realizations, or equivalently, over time $t = n\tau$ with $n \rightarrow \infty$. The eigenvalues of the average response tensor determine the dispersion relation, which yields the growth rate (γ) and cycle period (P_{cyc}) of growing mean-field dynamo wave. Below we first list some key properties and assumptions of our model:

- Shear rate S and velocity correlation time τ are the arbitrary parameters. We have ignored the diffusion term from the induction equation in this work to keep the analysis simpler.
- Helical shearing waves that were used to model the renovating flow freely evolve for the renovation time interval τ , and are reset to the same amplitude at the beginning of each renovation interval. The parameters of the flow take random values in different intervals such that the velocity field becomes completely uncorrelated after time τ . Such a model of the flow tries to capture the effects of stochastic helical forcing after every τ .

We studied the properties of growth rate and cycle periods of growing large-scale magnetic fields that are obtained by a mean-field dynamo action due to helical stochastic flows in a background linear shear. We focused in the regime when memory effects become important, i.e., when the response tensor or the turbulent EMF is affected by the time dependence of the mean magnetic field. As clarified in Sridhar & Singh (2014), this is equivalent to the case when the random flows are correlated for non-zero times, as in the white-noise case the generalized EMF with a history term through a time-integral reduces to a simple expression leading to an instantaneous relation with the mean magnetic field. Our study thus essentially generalizes the standard $\alpha^2\Omega$ dynamo model to now also include the memory effects, and tensorial nature of α while treating the shear non-perturbatively.

(a) *Non-axisymmetric ($k_2 \neq 0$) modes:* We found that the non-axisymmetric modes eventually decay in time and therefore are unimportant for late time structures of mean magnetic field. However, these modes decay in an interesting manner in that the contours of the growth rate γ form an ellipse with properties resembling the one for resistive Green's function which is derived by Sridhar & Singh (2010) for nonzero η after ignoring the advection term. As we have ignored η in the present work, the resemblance points to a notion of turbulent diffusivity η_t which typically augments η . The decay of such non-axisymmetric modes may thus be used to determine η_t and this will be attempted in a future work.

(b) *Axisymmetric ($k_2 = 0$) modes:* These are the only modes that survive and will determine the late time evolution of mean magnetic field. Comparing our results of axisymmetric mean field dynamo with the predictions of standard $\alpha\Omega$ dynamos, we find that the behaviours of γ and P_{cyc} with shear strength $|S|$ are even qualitatively different when $\tau/T \sim \mathcal{O}(1)$. Some notable findings in the regime when memory effects become important, i.e. when $\tau/T \sim \mathcal{O}(1)$, are highlighted as follows:

(i) The growth rate γ and the wavenumber (k_*) corresponding to the fastest growing mode vary non-monotonically with $|S|$; see Figures 4 and 6. We find the quenching of the dynamo when shear becomes sufficiently strong. This is in agreement with the work of Leprovost & Kim (2008) who also reported dynamo quenching due to strong shear. Common notions that the regions of strongest shear in an astrophysical object are the ideal reservoirs of magnetic fields may thus need to be revised.

In order to understand the cause of such a quenching of growth rate (γ), we made an attempt to determine the α tensor by adapting to its simplified textbook definition. We found that the magnitude of the more relevant component α_{22} is significantly suppressed at larger shear and this may have affected the growth of mean magnetic field.

(ii) At fixed S and τ , γ first increases from zero as a function of wavenumber, reaches a maximum, and turns negative at much larger wavenumbers. The quantity k_* is smaller than q , which is the eddy wavenumber determining the injection scale (q^{-1}) of kinetic energy, for a whole range of shear. Also, at fixed shear, k_* systematically decreases when τ increases. This promotes a genuine large-scale dynamo as magnetic fields grow maximally at scales (k_*^{-1}) that are larger than eddy size (q^{-1}).

(iii) Dynamo cycle period P_{cyc} exhibits different scaling relations with shear depending on the strength of the shear parameter: $P_{\text{cyc}} \propto |S|^{-1}$ when shear is small, and it becomes independent of shear when shear becomes sufficiently strong. This is very different from the predictions of standard $\alpha\Omega$ dynamo model which leads to a uniform scaling, $P_{\text{cyc}} \propto |S|^{-1/2}$, with shear.

Recent observational study by Olsper et al. (2018) on stellar magnetic activity cycles reveal two branches, active and inactive, in a diagnostic activity-rotation diagram. More work is needed to fully understand the origin of these branches, e.g., whether these trace two distinct population of stars or are somehow related to multiple cycles from the same star. Nevertheless, such studies emphasize the need to focus on the dynamo cycle period P_{cyc} as this may have direct implications for these observations. This motivated us to explore in detail the properties of P_{cyc} in our model. Interestingly enough, we find two asymptotic branches when we look at the dimensionless quantity $1/|S|P_{\text{cyc}}$; see the inset of Figure 8. This quantity is independent of shear when shear is weak, and varies as $|S|^{-1}$ in the strong shear regime. It is useful to note that the model predictions and scaling relations such as the ones reported here are often based on kinematic analysis, whereas the observations relate to the nonlinear stage of stellar dynamos. Therefore it is important to investigate numerically how the scalings of P_{cyc} are affected in the nonlinear stage. Nevertheless, we envisage that the new scaling laws being reported here will be useful in the interpretations of observations of the magnetic activity cycles of stars.

ACKNOWLEDGMENTS

We thank the referee for useful comments and suggestions. We thank S. Sridhar for useful discussions and comments on the manuscript. We thank Axel Brandenburg and Tarun Deep Saini for their support. NJ acknowledges the hospitality provided by Nordita, Sweden, where this work began. NJ also thanks Chanda J. Jog for providing financial support.

REFERENCES

- Bayly, B. J. & Childress, S., 1988, *Geophys. Astrophys. Fluid Dynamics*, **44**, 211
- Bhat, P. & Subramanian, K., 2015, *Journal of Plasma Physics*, **81**, 5
- Brandenburg, A., Bigazzi, A. & Subramanian, K., 2001, *Mon. Not. R. Astr. Soc.*, **325**, 685–692
- Brandenburg, A., & Subramanian, K., 2005, *Physics Reports*, **417**, 1–209.
- Brandenburg, A., Rädler, K.-H., Rheinhardt, M. & Käpylä, P. J., 2008, *ApJ*, **676**, 740–751.
- Brandenburg, A., Sokoloff, D., & Subramanian, K., 2012, *Spa. Sci. Rev.*, **169**, 123–157.
- Chamandy, L., & Singh, N. K., 2017, *Mon. Not. R. Astr. Soc.*, **468**, 3657
- Charbonneau, P., 2010, *Liv. Rev. Sol. Phys.*, **7**, no 3.
- Courvoisier, A., Hughes, D. A. & Tobias, S. M., 2006, *Physical Review Letters*, **96**, 034503.
- Dormy, E. & Soward, A. M., *Mathematical Aspects of Natural Dynamos*, CRC Press (2007)
- Du, Y., & Ott, E., 1993, *Journal of Fluid Mechanics*, **257**, 265–288
- Finn, J. M., & Ott, E., 1988, *Physics of Fluids*, 31(**10**), 2992
- Gilbert, A. D., & Bayly, B. J., 1992, *Journal of Fluid Mechanics*, **241**, 199 (GB92).
- Goldreich, P. & Lynden-Bell, D., 1965, *Mon. Not. R. Astr. Soc.*, **130**, 125.
- Gressel, O., Elstner, D., Ziegler, U. & Rüdiger, G., 2008, *Astron. & Astrophys.*, **486**, L35
- Han, J. L., 2017, *Ann. Rev. of Astron. and Astrophys.*, **55**, 111–157.
- Hori, K. & Yoshida, S., 2008, *Geophys. Astrophys. Fluid Dynamics*, **102**, 601
- Jones, C. A., 2011, *Annual Review of Fluid Mechanics*, **43**, 583
- Jingade, N. & Singh, Nishant K., 2020, Paper II in preparation
- Käpylä, P. J., Mantere, M. J., & Brandenburg, A., 2012, *Astrophys. J. Lett.*, **755**, L22
- Käpylä, M. J., Käpylä, P. J., Olsper, N., Brandenburg, A., Warnecke, J., Karak, B. B., & Pelt, J., 2016, *Astron. & Astrophys.*, **589**, A56
- Käpylä, M. J., Gent, F. A., Väisälä, M. S., & Sarson, G. R., 2018, *Astron. & Astrophys.*, **611**, A15
- Kleeorin, N., & Rogachevskii, I., 2003, *Physical Review E*, **67**, 026321.
- Lundquist, S., 1951, *Physical Review*, **83**, 307.
- Kolekar, S., Subramanian, K., & Sridhar, S., 2012, *Phys. Rev. E*, **86**, 026303 (KSS12).
- Kraichnan, R. H., 1976, *Journal of Fluid Mechanics*, **75**, 657.
- Kraichnan, R. H., 1976, *Journal of Fluid Mechanics*, **77**, 753.
- Krause, F. & Rädler, K.-H., *Mean-field magnetohydrodynamics and dynamo theory*; Pergamon Press, Oxford (1980).
- Leprovost, N. & Kim, E., 2008, *Physical Review Letters*, **100**, 144502.
- Mitra, D., Käpylä, P. J., Tavakol, R., & Brandenburg, A., 2009, *Astron. & Astrophys.*, **495**, 1
- Moffatt, H. K., *Magnetic Field Generation in Electrically Conducting Fluids*; Cambridge University Press, Cambridge (1978).
- Molchanov, S. A. and Ruzmaikin, A. A. & Sokolov, D. D., 1984, *Geophysical and Astrophysical Fluid Dynamics*, **30**, 241
- Molchanov, S. A., Ruzmaikin, A. A. & Sokolov, D. D., 1985, *Sov. Phys. Usp.* **28**, 307.
- Olsper, N., Lehtinen, J. J., Käpylä, M. J., Pelt, J., & Grigorievskiy, A., 2018, *Astron. & Astrophys.*, **619**, A6
- Dittrich, P., Molchanov, S. A., Sokoloff, D. D. & Ruzmaikin, A. A., 1984, *Astronomische Nachrichten*, **305**, 3, 119–125
- Hoyng, P., 1987, *Astron. & Astrophys.*, **171**, 357–367
- Parker, E. N., *Cosmical magnetic fields: Their origin and their activity*; Clarendon Press, Oxford; Oxford University Press, New York (1979).
- Rädler, K.-H., Kleeorin, N., & Rogachevskii, I., 2003, *Geophysical. and Astrophysical. Fluid Dynamics*, **97**, 249
- Ruzmaikin, A. A., Shukurov, A. M. & Sokoloff, D. D., *Magnetic Fields of Galaxies*; Kluwer, Dodrecht (1998)
- Schekochihin, A. A., Boldyrev, S. A. & Kulsrud, R. M., 2002, *ApJ*, **567**, 828.
- Singh, N. K. & Sridhar, S., 2011, *Physical Review E*, **83**, 056309.
- Singh, N. K. & Sridhar, S., 2017, *Eur. Phys. J. Plus*, **132**, 403.
- Sridhar, S. & Singh, N. K., 2010, *Journal of Fluid Mechanics*, **664**, 265.
- Sridhar, S. & Singh, N. K., 2014, *Mon. Not. R. Astr. Soc.*, **445**, 3770.
- Sridhar, S. & Subramanian, K., 2009, *Physical Review E*, **80**, 066315(1)–066315(13).
- Sur, S., Brandenburg, A., & Subramanian, K., 2008, *Mon. Not. R. Astr. Soc.*, **385**, L15
- Viviani, M., Käpylä, M. J., Warnecke, J., Käpylä, P. J. & Rheinhardt, M., 2019, eprint arXiv:1902.04019
- Warnecke, J., Käpylä, P. J., Käpylä, M. J., & Brandenburg, A., 2014, *Astrophys. J. Lett.*, **796**, L12
- Zeldovich, Ya. B., Ruzmaikin, A. A., & Sokoloff, D. D., *Magnetic fields in astrophysics*, Gordon & Breach, New York (1983)
- Zeldovich, Ya. B., Ruzmaikin, A. A., Molchanov, S. A. & Sokoloff, D. D., 1984, *J. Fluid Mech.*, **144**, 1–11.

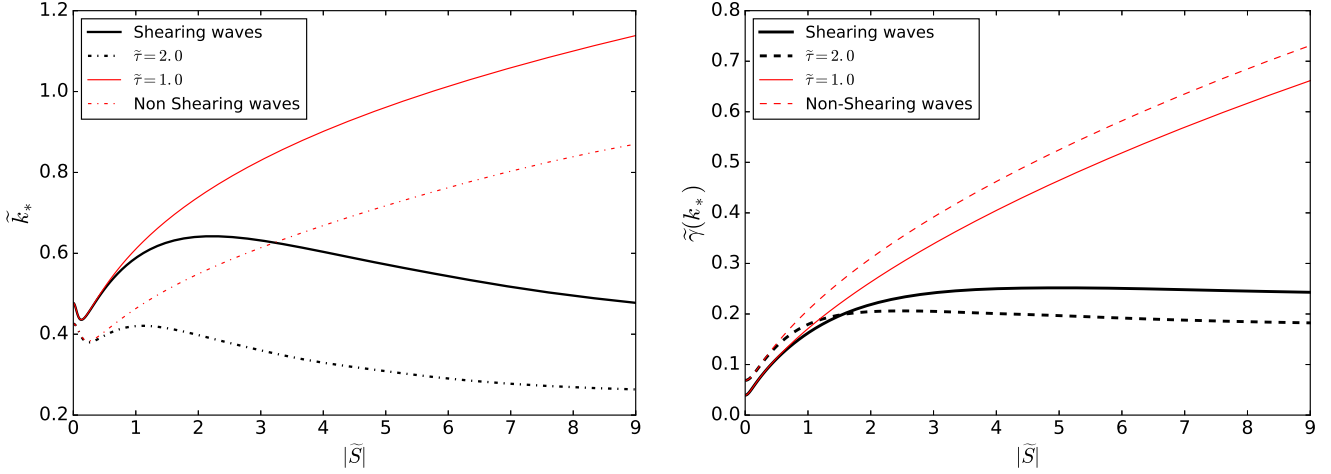


Figure A1. Normalized growth rate $\tilde{\gamma}(k_*)$ and normalized maximum growing mode k_* of growing dynamo are shown in left and right panels, respectively. Black: shearing waves; red: non-shearing waves; $\tau/T = 1$ (solid), and 2 (dashed)

APPENDIX A: COMPARISON WITH NON-SHEARING WAVES OF THE RENOVATING FLOWS

We choose the turbulent velocity \mathbf{u} same as in GB92,

$$\mathbf{u}(\mathbf{X}, t) = \mathbf{a} \sin(\mathbf{q} \cdot \mathbf{X} + \Psi) + h \mathbf{c} \cos(\mathbf{q} \cdot \mathbf{X} + \Psi) \quad (\text{A1})$$

which is a single helical waves with constant wave vector \mathbf{q} and constant amplitudes \mathbf{a} and \mathbf{c} . We call them *non-shearing waves*, since both the amplitudes and the wave vector are independent of shear. This velocity field is used instead of Eq. (2) to obtain the growth rate (γ) and maximum growing wavenumber (k_*). Such velocity field give, isotropic transport co-efficient $-\alpha$, if we use Eq. (34). This velocity fields are used, so that we can make the comparison between the cases, when α is tensorial and a function of shear, with isotropic α —independent of shear—in this appendix. The effect of shear on the turbulent eddy is not considered in the non-shearing waves as it is usually the case in $\alpha\Omega$ ($\alpha^2\Omega$) dynamo.

We show such comparisons in Figure A1 at $\tau/T = 1$ and 2, when memory effects are important. As may be seen from Figure A1 (left panel) that the behaviour of the wavenumber k_* corresponding to the fastest growing dynamo mode is qualitatively different. When we model renovating flows in terms of non-shearing waves, k_* increases with $|S|$, producing magnetic fields predominantly at small, sub-eddy spatial scales at intermediate to large values of shear (red lines). However, as discussed before based on Figure 4, when we consider amplitude modulated shearing waves in the model, we find that k_* remains small at all shear, thus producing magnetic fields preferentially at large, super-eddy spatial scales (black lines). Note that the background shear operates at all times, regardless of which one of the two, shearing or non-shearing, waves we use to model the renovating flows.

In Figure A1 (right panel) we show the comparison for shear dependence of the dynamo growth rate again at $\tau/T = 1$ and 2. While the growth rate $\tilde{\gamma}(k_*)$ increases monotonically with shear strength $|S|$ when non-shearing waves are used in calculations, it shows a saturation and even quenching at large enough values of shear when we utilize time-dependent shearing waves to model the renovating flows; dynamo quenching in strong shear regime is more clearly seen in Figure 6 where shear strength is shown on a logarithmic axis. Here, we have considered the growth of mean field by the single eddy with and without the effect of shear on its amplitudes along with the background flow. Therefore, the effect of shear on the turbulence is non-trivial which cannot be neglected and it is more pronounced at strong shear regime.